Nuclear Magnetic Resonance Studies of Some *N*′-Substituted Pyridine-2-carbaldimine Adducts of n-Butyltrichlorotin(IV) and the Molecular Structure of n-Butyltrichloro(*N*′-phenylpyridine-2-carbaldimine-*NN*′)-tin(IV)

By **Gen-etsu Matsubayashi** and **Toshio Tanaka,*** Department of Applied Chemistry, Faculty of Engineering, Osaka University, Suita, Osaka 565, Japan
Satoshi Nishigaki and **Kazumi Nakatsu,*** Faculty of Science, Kwansei Gakuin University, Nishinomiya, Hyogo 662, Japan

Six-co-ordinate n-butyltrichlorotin(IV) adducts with some *N*′-substituted pyridine-2-carbaldimines, $SnBu^nCl_3 \cdot C_5H_4N(CH{=}NR)$ (R = Me, Et, CH_2Ph, Bu^t, Ph, C_6H_4Me-*p*, or C_6H_4OMe-*p*), have been isolated. When the substituent (R) on the imine nitrogen atom is Me, Et, or CH_2Ph the adduct exists as a mixture of two isomers in acetonitrile, and when R = Bu^t or the other aryl groups only one species exists. The configuration of these isomers is proposed on the basis of the ^1H chemical shifts of the ligand protons and their spin–spin coupling constants with the tin nuclei. In addition, the molecular structure of the adduct with R = Ph has been determined by single-crystal *X*-ray diffraction. The triclinic crystal, space group $P\bar{1}$, has cell dimensions a = 8.655(8), b = 13.984(10), c = 8.662(5) Å, α = 102.16(7), β = 104.15(7), γ = 102.97(7)°, and Z = 2. Least-squares refinement of 2 764 independent reflections has given an R factor of 0.027.

SPIN–SPIN coupling constants between ^{117}Sn and/or ^{119}Sn nuclei and ligand protons in halogeno-organotin(IV) adducts with Lewis bases should give information on the configuration of the adducts. However, there have been only limited reports [1-3] on the determination of the configuration of organotin adducts in solution on the basis of ligand proton–tin coupling constants. This is partly because in solution the adducts often dissociate partly into the halogeno-organotin and ligand molecules and the free and complexed ligands exchange rapidly, resulting in no observation of the ligand proton–tin coupling. Recently, we have found that some pyridine-2-carbaldimine (1) adducts of $SnBu^nCl_3$ are fairly soluble

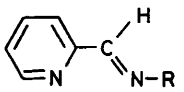

(1)

R = Me, Et, CH_2Ph, Bu^t, Ph, C_6H_4Me-*p*, or C_6H_4OMe-*p*

in acetonitrile without dissociation and that in the ^1H n.m.r. spectra the NCH_3, NCH_2, H_a, and H^6 signals are accompanied by satellites due to couplings between these protons and the tin nuclei. This paper reports the ^1H n.m.r. spectra of these adducts in acetonitrile revealing their configurations. The molecular structure of n-butyltrichloro(*N*′-phenylpyridine-2-carbaldimine)-tin(IV) has also been determined by means of *X*-ray crystallographic analysis.

EXPERIMENTAL

Preparations of the Adducts.—*N*′-Substituted pyridine-2-carbaldimines were obtained by reaction of pyridine-2-carbaldehyde and the corresponding alkyl- or aryl-amines as described previously.[1] A diethyl ether solution of $SnBu^nCl_3$ was mixed with a slight excess of the carbaldimine in the same solvent to give the 1 : 1 adduct as a precipitate, which was recrystallized from a mixture of light petroleum (b.p. 30—50 °C) and dichloromethane. Elemental analyses and properties of the adducts are listed in Table 1. The adducts, white or pale yellow, are stable in air.

Physical Measurements.—Molecular weights were determined in acetonitrile at 37 °C using a Mechrolab vapour-pressure osmometer. Electric conductivities of the *N*′-methyl- and *N*′-*p*-methoxyphenyl-pyridine-2-carbaldimine adducts were determined in acetonitrile at 25 °C, using a Universal bridge, as 1.3 (3.09×10^{-3}) and 0.67 S cm^2 mol^{-1} (1.87×10^{-3} mol dm^{-3}), respectively. Hydrogen-1 n.m.r. spectra were recorded on a Japan Electron Optics JNM-PS-100 spectrometer operating at 100 MHz against tetramethylsilane as internal standard. The chemical shifts and spin-spin coupling constants between ^{117}Sn and/or ^{119}Sn nuclei and ligand protons were measured with an accuracy of ±0.01 p.p.m. and ±1 Hz, respectively.

TABLE 1

Melting points, elemental analyses,[a] and molecular weights [a,b] of $SnBu^nCl_3 \cdot C_5H_4N(CH{=}NR)$

		Analysis (%)			
Adduct	M.p. (θ_c/°C)	C	H	N	*M*
R = Me	148—149	32.65	4.15	7.00	384
		(32.85)	(4.25)	(6.95)	(402)
Et	162—164	34.35	4.40	6.90	400
		(34.6)	(4.60)	(6.75)	(416)
CH_2Ph	119—122	42.3	4.40	6.00	472
		(42.7)	(4.45)	(5.85)	(478)
Bu^t	160—163	37.6	5.25	6.55	*c*
		(37.85)	(5.20)	(6.30)	
Ph	203	41.15	4.15	6.10	477
		(41.4)	(4.10)	(6.05)	(465)
C_6H_4Me-*p*	207	42.4	4.35	5.95	482
		(42.7)	(4.45)	(5.85)	(478)
C_6H_4OMe-*p*	205	41.2	4.35	6.00	509
		(41.3)	(4.35)	(5.65)	(494)

[a] Calculated values are given in parentheses. [b] In acetonitrile. [c] Decomposed in acetonitrile at elevated temperatures.

Collection of X-*Ray Diffraction Data.*—Single crystals of $SnBu^nCl_3 \cdot C_5H_4N(CHNPh\text{-}2)$ were obtained from an acetonitrile solution as pale yellow plates. A specimen with dimensions 0.10 × 0.12 × 0.15 mm was sealed in a glass capillary. The space group and approximate cell parameters were determined from oscillation and Weissenberg photographs.

A computer-controlled Rigaku four-circle diffractometer with graphite-monochromatized Mo-K_α (λ 0.710 69 Å)

TABLE 2

Atomic co-ordinates ($\times 10^4$; H, $\times 10^3$) with estimated standard deviations in parentheses

Atom	x	y	z
Sn	3 004.1(3)	2 119.7(2)	2 665.1(3)
Cl(1)	3 330(1)	382.9(8)	2 518(1)
Cl(2)	2 101(2)	3 644.6(9)	3 235(2)
Cl(3)	1 495(2)	1 626(1)	−272(1)
N(1)	609(4)	1 416(2)	3 191(4)
N(2)	3 612(4)	2 302(2)	5 492(4)
C(1)	−880(5)	980(3)	2 036(5)
C(2)	−2 309(5)	654(4)	2 473(6)
C(3)	−2 207(5)	768(4)	4 102(6)
C(4)	−665(5)	1 191(4)	5 294(6)
C(5)	720(5)	1 517(3)	4 793(5)
C(6)	2 397(5)	1 967(3)	5 987(5)
C(7)	5 270(5)	2 667(3)	6 649(5)
C(8)	6 240(6)	3 638(3)	6 835(6)
C(9)	7 846(6)	3 979(4)	7 917(7)
C(10)	8 486(6)	3 333(4)	8 751(6)
C(11)	7 514(6)	2 380(4)	8 542(6)
C(12)	5 889(5)	2 034(3)	7 476(6)
C(13)	5 465(6)	2 738(4)	2 585(6)
C(14)	5 824(10)	3 837(5)	2 353(11)
C(15)	7 525(12)	4 349(6)	2 672(15)
C(16)	7 532(15)	5 382(6)	2 075(15)
H(1)	−100(5)	88(3)	83(5)
H(2)	−346(6)	36(4)	154(6)
H(3)	−321(6)	52(4)	444(6)
H(4)	−61(6)	130(4)	647(7)
H(6)	268(5)	204(3)	720(5)
H(8)	581(6)	406(4)	621(6)
H(9)	838(7)	467(4)	789(7)
H(10)	948(6)	358(4)	965(6)
H(11)	790(6)	191(4)	925(6)
H(12)	507(5)	139(3)	727(5)
H(13–1)	611(6)	271(4)	342(6)
H(13–2)	555(6)	228(4)	171(6)

radiation was used for the measurement of diffraction intensities. The cell constants and their standard deviations were determined by least-squares treatment of the angular co-ordinates of 25 independent reflections with 2θ values from 30 to 36°.

Crystal data. $C_{16}H_{19}Cl_3N_2Sn$, $M = 464.4$, Triclinic, space group $P\bar{1}$, $a = 8.655(8)$, $b = 13.984(10)$, $c = 8.662(5)$ Å, $\alpha = 102.16(7)$, $\beta = 104.15(7)$, $\gamma = 102.97(7)°$, $U = 950.7(14)$ Å^3, D_m(flotation) = 1.62 g cm^{-3}, $Z = 2$, $D_c = 1.623$ g cm^{-3}.

Intensity data were collected for the hemisphere defined by h, $\pm k$, $\pm l$ up to $2\theta = 55°$ using the ω—2θ scan technique with a scan rate in ω of 1° min^{-1}. 3 349 Independent intensities were recorded, of which 2 764 had intensities larger than three times their standard deviations, and were used in the subsequent calculations. Throughout the data collection the intensities of five reference reflections were measured after every 50 reflections.

Structure determination and refinement. The space group $P\bar{1}$ assumed for the crystal was confirmed by a successful solution of the structure. The co-ordinates of the tin atom were found from a three-dimensional Patterson synthesis. All the least-squares refinements in this analysis were carried out on F, the function minimized being $\Sigma w(|F_o| - |F_c|)^2$ and the weights w being taken as $1/\sigma^2(F_o) + 0.000\,5|F_o|^2$ at the final cycle. A Fourier synthesis established the positions of the remaining non-hydrogen atoms, which complied with the chemically expected model. Four cycles of block-diagonal least-squares refinement reduced R from 0.36 to 0.070, assuming anisotropic temperature factors for the tin and three chlorine atoms. At this stage, the temperature factors for C(14), C(15), and C(16) (see the labelling in Figure 4) were found to be large. A difference-Fourier map based on anisotropic refinement of all the non-hydrogen atoms contained electron densities in positions which could be attributed to pyridine- and phenyl-ring hydrogen atoms and to hydrogen atoms attached to C(6) and C(13). The hydrogen atoms attached to C(14), C(15), and C(16) were omitted from the refinement because they could not be located with any certainty owing to large thermal vibrations of these carbon atoms. The block-diagonal least-squares refinement with anisotropic thermal parameters for all the non-hydrogen atoms and with isotropic thermal parameters for hydrogen atoms except for those attached to C(14), C(15), and C(16) led to final error indices $R = \Sigma||F_o| - |F_c||/\Sigma|F_o| = 0.027$ and $R' = [\Sigma w(|F_o| - |F_c|)^2/\Sigma w|F_o|^2]^{\frac{1}{2}} = 0.036$. The final difference-Fourier map showed

TABLE 3

Relevant ^{1}H n.m.r. data of $SnBu^nCl_3{\cdot}C_5H_4N(CH{=}NR)$ in acetonitrile at 24 °C [a]

R	Configuration	H^3	H^4	H^5	H^6	H_a	Other protons
Me [b]	(2)				9.60 [33] (1.00)	8.75 [*c*] (0.4)	3.75 [15] (NCH_3) (0.21)
	(3)				8.80 [7] [d] (0.20)	8.75 [*c*] (0.4)	3.85 [36] (NCH_3) (0.31)
Et [b]	(2)				9.74 [34] (1.11)	8.85 [*c*] (0.5)	4.04 [*c*] (NCH_2) (0.37)
	(3)				8.85 [4] [d] (0.2)	8.85 [*c*] (0.5)	4.27 [*c*] (NCH_2) (0.6)
CH_2Ph	(2)				9.65 [33] (1.01)	8.64 [15] (0.15)	5.22 [9] (NCH_2) (0.40)
	(3)				8.81 [9] [d] (0.17)	8.3 [102] [d] (−0.2)	5.43 [24] (NCH_2) (0.61)
Bu^t	(2)	8.15 (0.21)	8.37 (0.62)	7.99 (0.67)	9.72 [29] (1.04)	8.76 [14] (0.46)	
Ph	(2)	8.19 (0.06)	8.42 (0.60)	8.10 (*c*)	9.72 [34] (1.08)	8.82 [9] (0.29)	
C_6H_4Me-*p*	(2)	8.23 (0.06)	8.45 (0.59)	8.09 (0.69)	9.75 [35] (1.17)	8.84 [11] (0.26)	2.45 (CH_3) 7.36 (NC_6H_4) (0.08) (0.16)
C_6H_4OMe-*p*	(2)	8.20 (0.04)	8.43 (0.58)	8.05 (0.68)	9.76 [38] (1.07)	8.82 [11] (0.19)	3.84 (OCH_3) 7.08, 7.46 (NC_6H_4) (0.04) (0.12) (0.14)

[a] Chemical shifts (δ/p.p.m.), coupling constants between the ^{117,119}Sn nuclei and protons in square brackets (Hz), and values of δ(complexed) − δ(free) in parentheses. [b] The H^{3-5} signals were not well resolved owing to the presence of two isomers. [c] The determination was difficult owing to complexity, low intensity of the signals, and/or obscuration by other signals. [d] Estimated values (±3) on the basis of the weight-averaged values obtained from the rapid rearrangement between the two isomers in the presence of excess of $SnBu^nCl_3$ (see text).

little variation (+0.5 to −0.2 e Å^{-3}) over most of the map. The only significant peak (1.1 e Å^{-3}) appeared near the C(14) atom.

Throughout the refinement the atomic scattering factors for Sn^{4+}, Cl^-, N^0, C^0, and H(bonded) were used.[4] The positional parameters derived from the last cycle of the least-squares refinement, together with their associated standard deviations, are presented in Table 2. Structure-factor tables and anisotropic thermal parameters are in Supplementary Publication No. SUP 22406 (14 pp.).*

RESULTS AND DISCUSSION

Configuration of the Adducts in Acetonitrile.—Figure 1 shows the ^{1}H n.m.r. spectra of *N'*-*p*-methoxyphenylpyridine-2-carbaldimine and its $SnBu^nCl_3$ adduct in acetonitrile at room temperature. The ring-proton signals move downfield upon complex formation, as observed in the pyridine-2-carbaldimine adducts of $SnMe_2Cl_2$,[1] and $PtCl_2$ and $PdCl_2$.[5] The adduct is essentially monomeric and a non-electrolyte in acetonitrile. Thus, three possible configurations, (2)—(4), are suggested for the adduct. We have previously demonstrated that the 2,2'-bipyridine (bipy) and 1,10-phenanthroline (phen) adducts of $SnBu^nCl_3$ in solution adopt the configuration containing the two non-equivalent nitrogen atoms owing to the n-butyl group being located on the N–Sn–N plane in octahedral geometry.[2,3] In view of the chelation mode of pyridine-2-carbaldimine being similar to bipy and phen, configuration (2) or (3) is reasonably suggested for the *N'*-*p*-methoxyphenylpyridine-2-carbaldimine adduct.

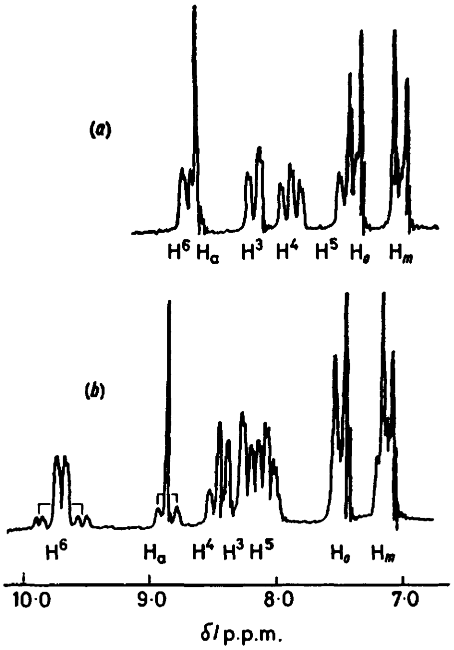

FIGURE 1 Hydrogen-1 n.m.r. spectra of (*a*) *N'*-*p*-methoxyphenylpyridine-2-carbaldimine and (*b*) its adduct with $SnBu^nCl_3$ in acetonitrile at 24 °C

It is well known that the spin–spin coupling constants of metal nuclei with protons located in a position *trans* to the metal atom with respect to carbon–nitrogen double bonds are larger than those with protons in the *cis* position.[5-8] In contrast, the coupling constants of the H_a proton with the tin nuclei [$^3J(Sn-H_a)$] are smaller than those of H^6 [$^3J(Sn-H^6)$], as shown in Table 3 (see also Figure 1). If one can relate a larger ^3J(Sn–H) value to a stronger nitrogen–tin bond this result may be explained by assuming configuration (2), in which the co-ordination of the imine nitrogen to the tin atom may be weaker than that of the pyridine nitrogen because of a possible repulsion between the n-butyl and *N'*-*p*-methoxyphenyl groups.

Similar configurations are suggested also for the *N'*-phenyl, *p*-tolyl, and t-butyl analogues on the basis of the weaker couplings of the tin nuclei with H_a than with H^6 (Table 3) related to their molecular weights. Configuration (2) in acetonitrile is compatible with the result of the *X*-ray analysis of the *N*-phenylpyridine-2-carbaldimine adduct, as described below.

The spectrum of the *N'*-benzylpyridine-2-carbaldimine adduct in acetonitrile is depicted in Figure 2, which shows two sets of signals due to the NCH_2, H_a, and H^6 protons, suggesting the presence of two isomers. It is to be noted that one of the H^6 signals occurred at a similar low field as that of the *N'*-*p*-methoxyphenyl adduct. In addition, the spin–spin coupling constant of H^6 with the tin nucleus is comparable with those in the *N'*-t-butyl and -aryl adducts. Thus, the lower-field H^6 signal may be associated with configuration (2). The NCH_2 signal in this configuration was observed at slightly higher field with a weaker tin coupling than that of the other NCH_2 signal (Table 3). This is suggestive of weaker co-ordination of the imine than the pyridine nitrogen atom to the tin. On the basis of the relative intensity of the NCH_2 signals, the concentration ratio [configuration (2): the other isomer] of the two isomers has been determined as 2.0 : 1 in acetonitrile.

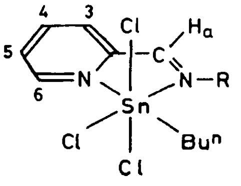

(2)

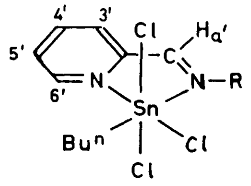

(3)

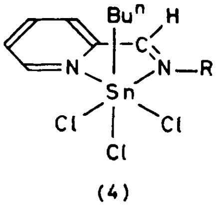

(4)

On the other hand, the downfield shift of the other H^6 signal ($H^{6'}$ in Figure 2) is not large. Tin-coupling satellites of the $H^{6'}$ signal have not been observed

---

* For details see Notices to Authors No. 7, *J.C.S. Dalton*, 1978, Index issue.

unequivocally owing to the weak intensities and/or overlapping of the signals. In the presence of excess of $SnBu^nCl_3$, however, an acetonitrile solution of the *N'*-benzylpyridine-2-carbaldimine adduct exhibited only one signal for each ligand proton, indicating rapid configurational rearrangement between two isomers, as seen in the bipy adduct of $SnBu^nCl_3$.[2] Under these conditions the $H^{6'}$ signal merged with the lower-field H^6 signal, giving a weight-averaged chemical shift of δ 9.40 p.p.m. and $^3J(Sn-H^6)$ of 25 Hz. Using $^3J(Sn-H^6)$ and averaged values together with the concentration ratio (2.0 : 1) of the two isomers, $^3J(Sn-H^{6'})$ has been estimated as 9 ± 3 Hz.* Such a small $^3J(Sn-H^{6'})$ value may be compatible with configuration (3), in which the repulsion between the pyridine ring and the n-butyl group may result in weakening of the pyridine nitrogen–tin bond. On the other hand, there may be no significant steric restriction between the imine nitrogen and the tin atom in configuration (3). In fact, the NCH_2 protons which appeared at lower field exhibited a larger spin–spin coupling constant with tin than those at higher field (Table 3).

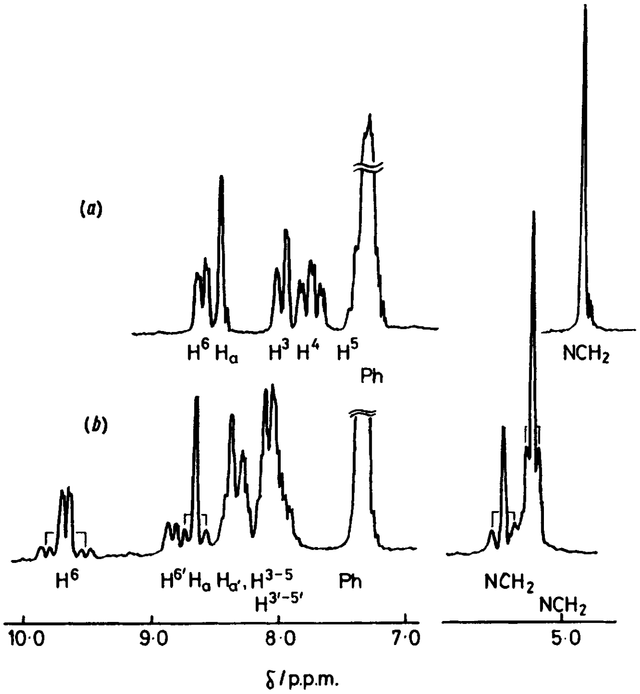

FIGURE 2 Hydrogen-1 n.m.r. spectra of (*a*) *N'*-benzylpyridine-2-carbaldimine and (*b*) its adduct with $SnBu^nCl_3$ in acetonitrile at 24 °C

The lower-field H_a signal with the satellites due to the tin coupling [$^3J(Sn-H_a)$ 15 Hz] was observed, while the higher-field one ($H_{a'}$) was obscured by other ring-proton signals (Figure 2). The spectrum in the presence of excess of $SnBu^nCl_3$ gave a weight-averaged $^3J(Sn-H_a)$ value of 44 Hz, from which the $^3J(Sn-H_{a'})$ value has been estimated as 102 ± 3 Hz. This is much larger than the $^3J(Sn-H_a)$ value. Thus, the lower (H_a) and higher field ($H_{a'}$) signals are assigned to configurations (2) and (3), respectively. The $^3J(Sn-H_{a'})$ value in configuration (3) may be compared with $^3J(^{195}Pt-H_a)$ (94—102 Hz) of *N'*-alkyl-and *N'*-aryl-pyridine-2-aldimine adducts with $PtCl_2$,[5] which would involve no significant steric repulsion between the *N*-substituents and the chlorine atom. The presence of two isomers for the *N'*-methyl and *N'*-ethyl adducts is similarly confirmed by the ^1H n.m.r. spectra. The concentration ratios of the two isomers [(2) : (3)] of these adducts in acetonitrile are 1.4 and 2.0 : 1 respectively.

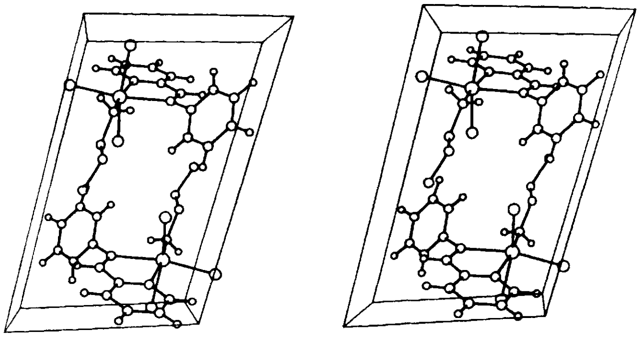

FIGURE 3 Stereoview of a unit cell of $SnBu^nCl_3 \cdot C_5H_4N(CHNPh-2)$. The origin of the cell is at the upper left corner. The *z* axis is horizontal, the *y* axis vertical, and the *x* axis points out from the corner

Molecular Structure of n-Butyltrichloro(N'*-phenyl-pyridine-2-carbaldimine*)*tin*(IV).—The crystal structure of the adduct consists of two discrete molecules per unit cell (Figure 3). A perspective view of the adduct along the *a** axis together with the labelling scheme is shown in Figure 4, and selected interatomic distances are given in Table 4. There are no unduly short intermolecular contacts in the unit cell. The adduct contains a six-co-

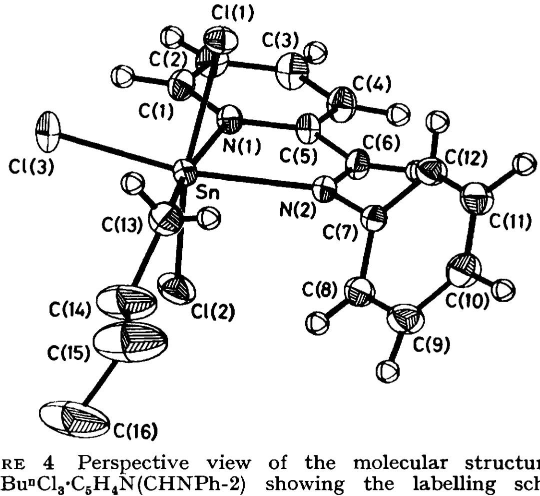

FIGURE 4 Perspective view of the molecular structure of $SnBu^nCl_3 \cdot C_5H_4N(CHNPh-2)$ showing the labelling scheme. Thermal ellipsoids are drawn at the 30% probability level except those for hydrogen atoms, which are represented by spheres having an arbitrary radius

---

* The validity of this estimation is supported by the fact that in the presence of excess of $SnBu^nCl_3$ only one NCH_2 signal was observed at δ 5.29 p.p.m. with a $^3J(Sn-NCH_2)$ value of 14 Hz, as the weight-averaged value of two $N-CH_2$ signals (see Table 3).

ordinate tin atom with two mutually **_trans_** chlorine atoms. The geometry, however, is deformed from a regular octahedron. The relative rigidity of the carbaldimine ligand and the large covalent radius of tin require the N(1)–Sn–N(2) bond angle to be <90°. Non-bonded repulsions of the n-butyl group with the Cl(3) atom and the N(2) phenyl group cause bond angles larger than 90° for Cl(3)–Sn–C(13) and C(13)–Sn–N(2). In addition, mutual repulsion of Cl(2) with C(13) opens the Cl(2)–Sn–C(13) angle to 101.6°. The Sn, N(1), N(2), Cl(3), and C(13) atoms are almost coplanar within a mean atomic deviation of 0.05 Å. Such a structure where the C(13) atom lies on this plane and near to N(2) is compatible with configuration (2) expected from the ^{1}H n.m.r. spectrum. The N(2)–Sn–C(13) angle is very large compared with the N(1)–Sn–Cl(3) angle, and the Sn–N(2) bond distance is slightly but significantly larger than the Sn–N(1) distance.

TABLE 4

Intramolecular distances (Å) and angles (°) with estimated standard deviations in parentheses

(*a*) Distances			
Sn–Cl(1)	2.488(2)	C(1)–C(2)	1.389(7)
Sn–Cl(2)	2.428(2)	C(2)–C(3)	1.364(7)
Sn–Cl(3)	2.426(2)	C(3)–C(4)	1.383(6)
Sn–N(1)	2.282(4)	C(4)–C(5)	1.387(7)
Sn–N(2)	2.320(4)	C(5)–C(6)	1.468(5)
Sn–C(13)	2.136(6)	C(13)–C(14)	1.564(9)
N(1)–C(1)	1.338(5)	C(14)–C(15)	1.415(12)
N(1)–C(5)	1.343(5)	C(15)–C(16)	1.633(15)
N(2)–C(6)	1.262(6)	C–C (phenyl, mean) *	1.380(6)
N(2)–C(7)	1.441(5)		
(*b*) Selected bond angles			
Cl(1)–Sn–Cl(2)	162.9(1)	Cl(3)–Sn–N(2)	161.4(1)
Cl(1)–Sn–Cl(3)	92.1(1)	Cl(3)–Sn–C(13)	99.6(2)
Cl(1)–Sn–N(1)	82.0(1)	N(1)–Sn–N(2)	71.6(1)
Cl(1)–Sn–N(2)	84.1(1)	N(1)–Sn–C(13)	169.7(2)
Cl(1)–Sn–C(13)	93.5(2)	N(2)–Sn–C(13)	98.8(2)
Cl(2)–Sn–Cl(3)	93.1(1)	N(1)–C(5)–C(6)	116.3(4)
Cl(2)–Sn–N(1)	81.7(1)	C(5)–C(6)–N(2)	119.7(4)
Cl(2)–Sn–N(2)	85.8(1)	C(6)–N(2)–C(7)	119.2(4)
Cl(2)–Sn–C(13)	101.7(2)	C(7)–N(2)–Sn	124.5(3)
Cl(3)–Sn–N(1)	89.9(1)		

* Defined as $\Sigma w_i y_i/\Sigma w_i$, where y_i is an individual C–C distance and w_i is the squared reciprocal of its standard deviation. The standard deviation of the mean is defined as $\{\Sigma w_i(y_i - \bar{y})^2/[(n - 1)\Sigma w_i]\}^{\frac{1}{2}}$.

The pyridine ring and the C(6), N(2), and C(7) atoms of the ligand are almost coplanar within a mean atomic deviation of 0.08 Å. However, the phenyl ring is twisted from this plane by 60.7°. The C(5)–C(6) [1.468(5) Å] and C(6)–N(2) bond lengths [1.262(6) Å] are comparable with those of metal complexes of related ligands: C–C 1.44(2) Å and C=N 1.28(2) Å for (*N*-methylsalicylaldiminato)(*N*-methylsalicylaldiminium)nickel(0);[9] C–C 1.46(2) and C=N 1.29(1) Å for bis(pyridine-2-carbaldoximinato)platinum(II) dihydrate.[7]

Since this is the first *X*-ray structure determination of six-co-ordinate monoalkyltrichlorotin(IV) adducts no comparative Sn–C bond distances are available. The Sn–Cl distances are very close to that of the six-co-ordinate mono-organotin complex chlorobis(*NN*-diethyldithiocarbamato)phenyltin(IV) [2.438(6) Å].[10] However, they are longer than those of a tetrachlorotin(IV) adduct, *cis*-$SnCl_4 \cdot 2MeCN$ [2.339(8), 2.341(7), 2.355(7), and 2.356(7) Å],[11] and shorter than those of a dichlorodiorganotin(IV) adduct, $SnPh_2Cl_2 \cdot$bipy [2.508(2) and 2.511(2) Å].[12] In the six-co-ordinate tin complexes partial replacement of chlorine atoms by less-electronegative organic groups causes an increase in the remaining Sn–Cl bond distances. This tendency is due to the preferential increase of *s* character in the Sn–C bonds and of the *p* and *d* characters in the remaining Sn–Cl bonds, as suggested previously.[13] The Sn–N distances of the present adduct are shorter than those of six-co-ordinate $SnPh_2Cl_2 \cdot$bipy [2.344(6) and 2.375(6) Å].[12] In view of the similarity in co-ordination mode between pyridine-2-carbaldimine and bipy, the difference may be partly due to the strong Lewis acidity of $SnBu^nCl_3$ compared with that of $SnPh_2Cl_2$.

[8/957 *Received*, 22*nd May*, 1978]

REFERENCES

[1] G. Matsubayashi, M. Okunaka, and T. Tanaka, *J. Organometallic Chem.*, 1973, **56**, 215.

[2] G. Matsubayashi and T. Tanaka, *J. Organometallic Chem.*, 1976, **120**, 347.

[3] G. Matsubayashi and J. Iyoda, *Bull. Chem. Soc. Japan*, 1977, **50**, 3055.

[4] ' International Tables for *X*-Ray Crystallography,' Kynoch Press, Birmingham, 1974, vol. 4.

[5] K. Kawakami, T. Ohara, G. Matsubayashi, and T. Tanaka, *Bull. Chem. Soc. Japan*, 1975, **48**, 1440.

[6] B. Crociani and R. L. Richards, *J.C.S. Dalton*, 1974, 693.

[7] K. W. Nordquest, D. W. Phelps, W. F. Little, and D. J. Hodgson, *J. Amer. Chem. Soc.*, 1976, **98**, 1104.

[8] L. Maresca, G. Natile, L. Cattalini, and F. Gasparrini, *J.C.S. Dalton*, 1976, 1090.

[9] M. Matsumoto, K. Nakatsu, K. Tani, A. Nakamura, and S. Otsuka, *J. Amer. Chem. Soc.*, 1974, **96**, 6777.

[10] P. G. Harrison, T. J. King, and J. A. Richards, *J.C.S. Dalton*, 1974, 1723.

[11] M. Webster and H. E. Blayden, *J. Chem. Soc.* (*A*), 1969, 2443.

[12] P. G. Harrison and A. Mangia, *J. Organometallic Chem.*, 1976, **120**, 211.

[13] H. A. Bent, *J. Inorg. Nuclear Chem.*, 1961, **19**, 43.